

Investigating slow shock in low-impedance materials using a direct impact Hopkinson bar setup

Puneeth Jakkula^{1,*}, Georg Ganzenmüller^{1,2,**}, Samuel Beisel¹, and Stefan Hiermaier^{1,2}

¹Albert-Ludwigs-Universität Freiburg, Sustainable Systems Engineering – INATECH, Emmy-noether-straße 2, 79110 Freiburg, Germany

²Fraunhofer Institute for High-Speed Dynamics, Ernst-Mach-Institut – EMI, Ernst-zermelo-straße 4, 79104 Freiburg, Germany

Abstract. This work implements a direct impact Hopkinson bar, suitable for investigating the evolution of dynamic force equilibrium in low-impedance materials. Polycarbonate as the bar material favours for a long pulse duration of 2.6 ms for an overall length of only 5 m, allowing to compress large specimens to high strains. This setup is applied to polyurethane foams with different densities ranging from 80 - 240 kg/m³. Dynamic compression tests are performed at strain rates of 0.0017, 0.5 and 500 /s on the foams at room temperature. Depending on density, they show a saturation in increase of yield strength at strain rates of 500 /s, or even show a negative strain rate sensitivity for the lowest density. This behaviour is explained by comparing the dynamic force equilibrium to a phenomenon similar to shock in solid materials: For low densities and high rates of strain, homogeneous compression is replaced by a localized collapse front with a jump in stress across the front. Digital image correlation is performed to analyse elastic and plastic compaction waves by means of Lagrange diagrams.

1 Introduction

Dynamic material testing of low density soft materials has traditionally been challenging [1]. It is difficult to achieve dynamic force equilibrium during the experiment to accurately measure the force. During the loading of a specimen, the stress state in the specimen requires a certain time to propagate through it, because the loading is only from one side. This time depends on the specimen dimensions and its material properties like wave speed c_0 . Additionally, the stress wave transmission and reflection depends on the ratio of acoustic impedance ($z = \rho c_0$, where ρ is mass density) to its mechanical boundaries [2].

Traditionally for dynamic material characterisation for metallic materials, Kolsky [3] setup has been proven very successful. However it reaches its limits when applied to low impedance materials: it is challenging to resolve the force amplitude due to low specimen strength using metallic bars, and it takes long time to reach dynamic force equilibrium because of the large impedance mismatch between specimen and the bar material. These problems can be addressed by switching to polymer bars. The smaller impedance mismatch increases the sensitivity of force measurement.

*e-mail: puneeth.jakkula@inatech.uni-freiburg.de

**e-mail: georg.ganzenmueller@inatech.uni-freiburg.de

Here a direct impact Hopkinson bar - Symmpact is employed with no separate striker as the input bar itself serves as the striker. The use of polymer bars (polycarbonate) together with short distances between strain gauges and specimen/bar interface, leads to negligible errors in force measurement due to wave attenuation and dispersion. The absence of dedicated strikers means two nearly identical waves travel into input and output bars. Thus avoiding the wave superposition of reflected and incident waves as found in classical split-Hopkinson pressure bars (SHPB). We note that we are not the first to pursue the general idea of having no striker: Govendar and Curry [4] tried similar setup with polymer bars, Hiermaier and Meenken [5] used metal bars but introduced piezoelectric foil gauges on both sides of the specimen to increase the force resolution.

We investigate polyurethane (PUR) foams with different densities in the range of 80 – 240 kg/m³. High density foams show a saturation of dynamic strength increase at high rates of strain ≥ 500 /s, or even negative strain rate sensitivity in case of the lowest density. The direct impact Hopkinson bar - Symmpact can measure the evolution of dynamic force equilibrium accurately and is used to explain this behaviour by linking it to a phenomenon similar to shock in solid materials: For low densities and high rates of strain, homogeneous compression is replaced by a localized collapse front with a jump in stress across the front.

2 Material and methods

2.1 Specimens

Thick plates of polyurethane foams of different densities were obtained in dimensions of 150 × 120 × 50 mm³ and are CNC milled to diameter \varnothing 30 mm and height 20 mm. Foams used in our work are Sikablock M80, M150 and M330 sold by Sika, Germany. These foams are manufactured by mixing polyols and isocyanates with water, resulting in a cross linking reaction which effects in release of CO₂ bubbles. Scanning electron microscope (SEM) images from Figure 1 show the transition of open cell to close cell structures as the density increases. The mechanical properties like density ρ , Young's modulus E , yield strength σ , and speed of sound $c_0 = \sqrt{E/\rho}$ according to the manufacturer are listed in Table 1.

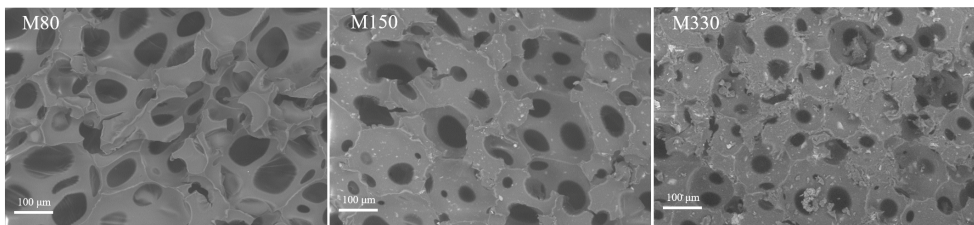


Figure 1: SEM images of freshly milled surfaces of Sikablock foams with 300X magnification.

Table 1: Mechanical properties of foams being investigated in this work.

foam	ρ [kg/m ³]	E [MPa]	σ [MPa]	c_0 [m/s]
M80	80	24	0.8	547
M150	150	65	2.2	658
M330	240	150	4.0	790

2.2 Quasi static testing

The quasi static compression tests were performed on the machine Zwick-Roell Z100 system with 100 kN load cell at room temperature. The load cell equipped with, is categorised under accuracy class 1 for forces < 200N. The cross-head velocities of the machine are chosen to achieve strain rates of 0.0017 /s and 0.5 /s. The specimen nominal strain was calculated from the displacement of the compression plates. A total of 5 specimens were tested at each strain rate, to check for the reproducibility of the milling quality of the specimen.

2.3 Dynamic testing with Symmpact

The direct impact Hopkinson bar - Symmpact, which has been implemented in this work is sketched in Figure 2. The input bar, which also serves as the striker is pneumatically accelerated in a cylindrical barrel. This barrel restricts the input bar's motion to one direct while providing space for strain gauges and their wirings. The barrel is a hollow aluminium profile (ITEM, Germany) of 2800 mm long and has an internal bore diameter of $\varnothing 40$ mm with a tolerance of +0.1/-0 mm. Both input and output bars are 2000 mm in length and made of polycarbonate (PC). Figure 3 shows two slots are cut in axial direction for the movement of strain gauges along the bar, this also provides a safe passage for the wires coming from strain gauges. To guide the output bar, short cut-offs of the same aluminium profile are used. The speed of sound c_0 being low in PC allows for a longer usable pulse duration of 2.6 ms.

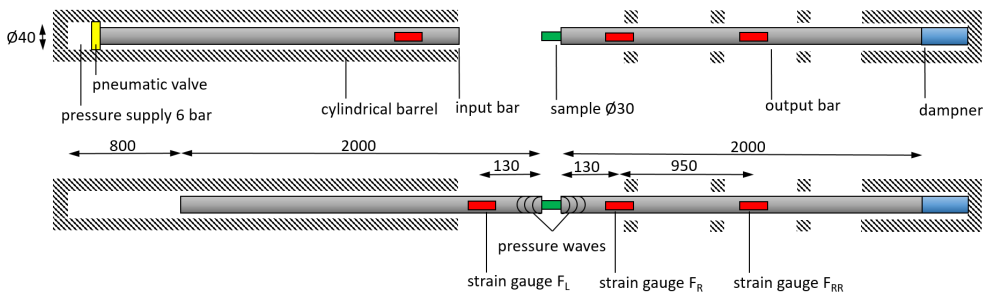


Figure 2: Sketch of Symmpact: a direct impact hopkinson bar used in this work. All dimensions are in mm.

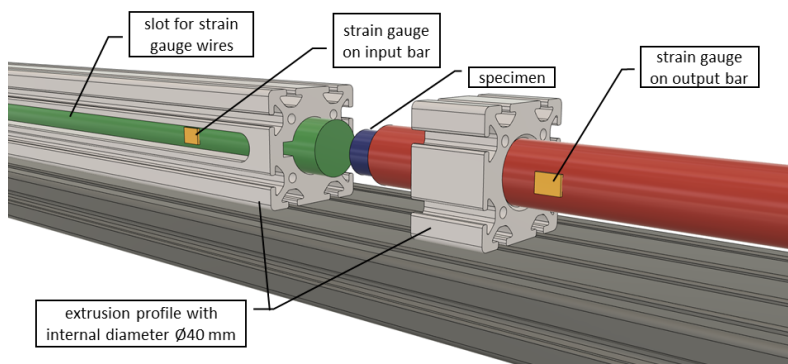


Figure 3: Detail of strain gauge access. The hollow extrusion profile features slots (one on each side) that provide access for the strain gauge wires (not shown here).

The significant advantage of the Symmpact setup over conventional split-Hopkinson pressure bar (SHPB) lies in the fact that nearly identical stress waves propagate into both input and output bars. As opposed to SHPB where the incident and reflected waves are superimposed. Figure 4 shows time evolution of force signals for an M150 specimen during initial 0.6 ms.

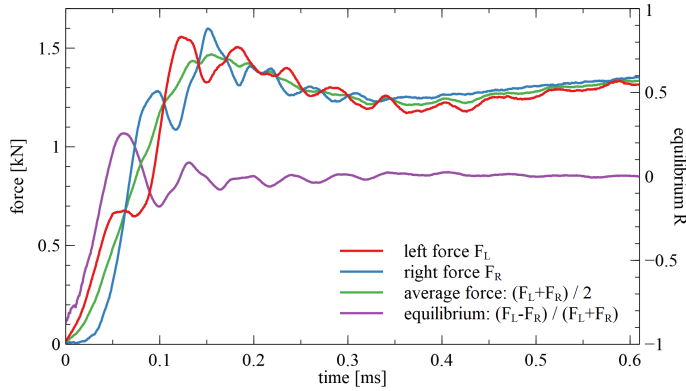


Figure 4: Individual force signals on input and output bar and their average as well as the ratio of forces indicating force equilibrium.

The reverberation period in the force signals matches well with the estimate, $\tau = 2L_0/c_0 = 0.06$ ms, where length $L_0 = 20$ mm and c_0 of specimen M150 from Table 1. The low noise level allows to use the average force expression, suitable to calculate the macroscopic stress in the specimen,

$$F_{avg} = \frac{F_L + F_R}{2} \quad (1)$$

This force estimate is the most accurate option to calculate the representative macroscopic stress from the strain gauge, as shown in the studies from Mohr *et al.* [6]. The oscillations due to reverberation cancel out each other, leading to an artefact free and smooth average signal. The evolution of dynamic equilibrium R is also well resolved.

3 Results

The stress strain data obtained for foams at different strain rates $\dot{\epsilon} = [0.0017, 0.5, 500]$ /s is shown in Fig. 5A. Five specimens were tested at each strain rate, but only two results are shown in the graph to avoid the clutter. The bar graph in Fig. 5B shows the average and standard deviation estimate of stress at strains of 0.1, 0.25 and 0.5 for foams. The measured values of stress agrees well with manufacturer’s data sheet as show in Table 1. All foam types show significant increase of $\approx 30\%$ in yield stress at 0.5 /s strain rate. Further increase to 500 /s strain rate, yield strength is improved in M150 and M330 but a drop in low-density M80 foam is observed. Fig. 5B compares stress values at strain $\epsilon = [0.1, 0.25, 0.5]$ for different strain rates to visualize this non-monotonic behaviour more clearly. In summary, we observe a negative strain rate sensitivity between 0.5 /s and 500 /s for low foam densities.

The base polymeric foam material – polyurethane, typically exhibits a monotonic positive strain-rate sensitivity until much higher rates of strain, as shown in [7]. To further investigate the possible structural effects that give rise to a negative strain rate sensitivity at low densities, the force equilibrium $R = (F_L - F_R)/(F_L + F_R)$ during strain rate of 500 /s, are plotted in

Fig. 6. Dynamic equilibrium is achieved within ≈ 0.5 ms for the highest-density foam, M330, whereas M80 requires ≈ 1.1 ms. Elastic wave reverberations can be identified for M330, but not for M80. As dynamic force equilibrium is linked to a homogeneous strain rate distribution via Newton’s acceleration law, these observations indicate non-homogeneous deformations in the case of the lower density foams.

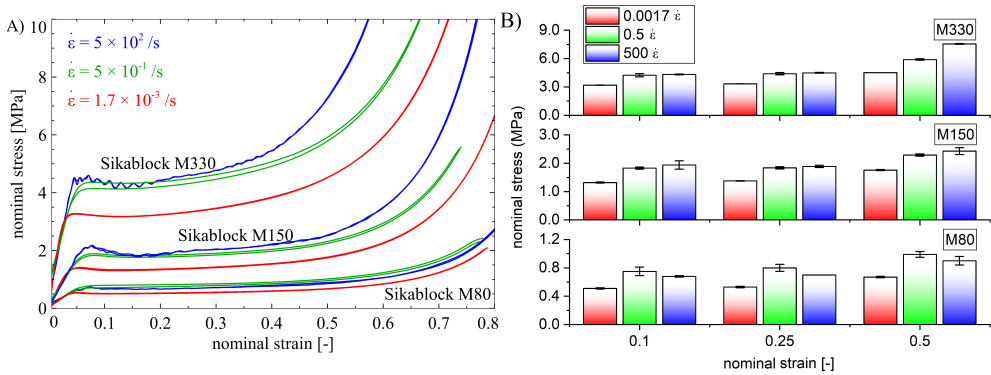


Figure 5: **A)** Stress-strain data for foams M80, M150 and M330 obtained at strain rates of 0.0017 /s, 0.5 /s, and 500 /s. **B)** compares stress values at three selected strain values, $\epsilon = 0.1$, 0.25, and 0.5, to emphasize the non-monotonic relation of stress to strain rate for the lower density foams M80 and M150.

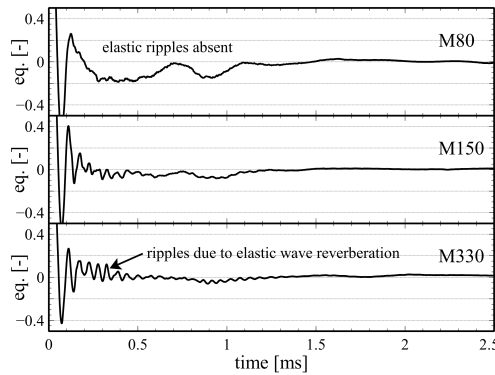


Figure 6: Evolution of dynamic equilibrium during loading at a strain rate of 500 /s.

The Lagrange diagrams in Fig. 7 shows three different foams compressed at 500 /s. Here, Digital Image Correlation (DIC) is used to extract the full-field strain rate measurements at every frame recorded at 360 KHz. These fields are then averaged along the radial direction of the specimen, assuming an axis-symmetric deformation field. The resulting line plots of strain rate vs. longitudinal position are stacked vertically, yielding a Lagrange diagram where time is on Y-axis and position is on X-axis. The local (both in space and time) amplitude of strain rate is visualized by blue colour. For M80, we initially observe a compression front travelling through the specimen at its c_0 ref. Table 1. The front is reflected on the right end and travels towards the left. Following this single reverberation, the strain rate

amplitude localizes at $t = 0.1$ ms and forms a localized compression front, which travels to the right at a much reduced velocity of ≈ 10 m/s. For M150, we observe a similar pattern, but two reverberations are visible. Strain rate localization then follows but is less pronounced. Whereas for M330, a much more homogeneous strain rate distribution is observed with many visible wave reverberations.

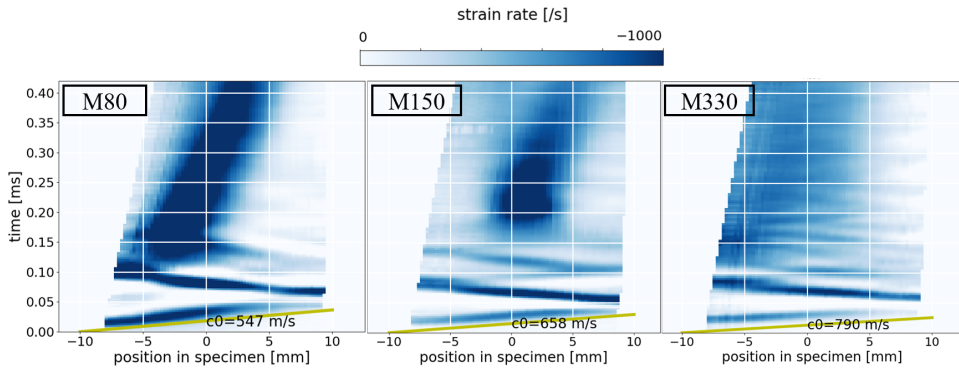


Figure 7: Lagrange plots of strain rate distribution in the foam specimens during dynamic compression at an average strain rate of 500 /s. Yellow lines at the bottom indicate the elastic speed of sound take from Table 1

4 Discussion and conclusion

The Symmpact setup presented here is particularly useful for investigating the evolution of dynamic force equilibrium. In contrast to conventional split-Hopkinson pressure bars, the advantage of having no wave superposition leads to comparatively accurate results for both the average force and dynamic force equilibrium. Here, we use a distance of 130 mm between specimen/bar interface and strain gauge, with bar diameter of 40 mm, resulting in estimated force measurement errors of less than 1% when compared to a reference dynamic load cell. For this setup, PC bars can be used just like metallic bars, only if strain gauges are placed close to the specimen/bar interface. Similar observations were made by Rao *et al.* [8].

Polyurethane (PUR) foam specimens with densities ranging from 80 - 240 kg/m³ are investigated. A strain rate increase from 0.0017 /s to 0.5 /s yields an increase of strength by $\approx 30\%$. However, a further increase of the strain rate to 500 /s is not accompanied by a further increase of strength: the lowest-density foam even shows a decrease in strength. In a similar study, Chen *et al.* [9] observed for rigid polyurethane foams that, while strain rate and strength are linked at low strain rates, no strain rate sensitivity exists in the regime 1000 /s to 5000 /s.

Here, we link the occurrence of a limit for the strain rate sensitivity a transition of the deformation behaviour to a structural shock regime: we propose that the homogeneous deformation observed at low rates of strain is replaced by a cell collapse mechanism, which travels as a macroscopic discontinuity through the specimen. This scenario bears some similarity to strong shock waves initiated at much higher impact velocities, $\approx 10^3$ m/s, in solid materials, but occurs here at much lower velocities, $\approx 10^1$ m/s (slow shock). In the strong shock wave scenario, the stress state upstream and downstream of the shock front is different. Similar observations have been made before for a low-density epoxy foam by Song *et al* [10]. Using a similar analysis as our Lagrange plots from Fig. 7, though with less resolution given the

technical possibilities at that time, they observed slow compaction waves travelling at ≈ 30 m/s in a material that has an elastic wave speed of ≈ 360 m/s. They argued that the compaction wave exhibits similarity to classic shock waves. In their analysis, the wavefront was treated as a discontinuity, and the shock Hugoniot relations were used to predict stress jumps across the wave front and, quite accurately, the locking density behind the compaction front.

The work presented here agrees with the interpretation of the travelling collapse front as a discontinuous shock-like wave. The lack of dynamic force equilibrium in low density foams supports the assumption of a discontinuity with different stress states downstream and upstream of the compaction front. Here, in case of the lower density foams M80 and M150, we observe the absence of force equilibrium for a pronounced period of time (Fig. 6), combined with a travelling localized compression front. Thus, we have a direct proof for the stress jump across the discontinuity, underlining the similarity to the strong shock regime and supporting the transition to a structural shock regime. In this regime, the foam is limited in its capability to further sustain stress because its structure breaks down locally.

5 Acknowledgement

We acknowledge the funding from Carl-Zeiss Foundation, grant title *Skalenübergreifende Charakterisierung robuster funktionaler Materialsysteme*.

References

- [1] Song, B.; Chen, W. Split Hopkinson Pressure Bar Techniques for Characterizing Soft Materials. p. 40.
- [2] Meyers, M.A. Dynamic Behavior of Materials; John Wiley and Sons.
- [3] Kolsky, H. An Investigation of the Mechanical Properties of Materials at Very High Rates of Loading. **62**, 676–700. doi:10.1088/0370-1301/62/11/302.
- [4] Govender, R.A.; Curry, R.J. The “Open” Hopkinson Pressure Bar: Towards Addressing Force Equilibrium in Specimens with Non-Uniform Deformation. **2**, 43–49. doi:10.1007/s40870-015-0042-2.
- [5] Hiermaier, S.; Meenken, T. Characterization of Low-Impedance Materials at Elevated Strain Rates. **45**, 401–409. doi:10.1243/03093247JSA584.
- [6] Mohr, D.; Gary, G.; Lundberg, B. Theoretical Assessment of Stress-Strain Curve Estimates in split Hopkinson Bar Experiments. DYMAT - International Conference on the Mechanical and Physical Behaviour of Materials under Dynamic Loading. EDP Sciences, Vol. **1**, pp. 485–490. doi:10.1051/dymat/2009069.
- [7] Sarva, S.S.; Deschanel, S.; Boyce, M.C.; Chen, W. Stress-Strain Behavior of a Polyurea and a Polyurethane from Low to High Strain Rates. **48**, 2208–2213. doi:10.1016/j.polymer.2007.02.058.
- [8] Rao, S.; Shim, V.P.W.; Quah, S.E. Dynamic Mechanical Properties of Polyurethane Elastomers Using a Nonmetallic Hopkinson Bar. **66**, 619–631. doi:10.1002/(SICI)1097-4628(19971024)66:4<619::AID-APP2>3.0.CO;2-V.
- [9] Chen, W.; Lu, F.; Winfree, N. High-Strain-Rate Compressive Behavior of a Rigid Polyurethane Foam with Various Densities. **42**, 65–73. doi:10.1007/BF02411053.
- [10] Song, B.; Forrestal, M.J.; Chen, W. Dynamic and Quasi-Static Propagation of Compaction Waves in a Low-Density Epoxy Foam. **46**, 127–136. doi:10.1007/s11340-006-5871-4.